Back action of nonequilibrium phonons on the optically induced dynamics in semiconductor quantum dots

A. Krügel, V. M. Axt, and T. Kuhn
Institut für Festkörpertheorie, Westfälische Wilhelms-Universität Münster, Wilhelm-Klemm-Str. 10, D-48149, Münster, Germany
(Received 9 August 2005; revised manuscript received 31 October 2005; published 3 January 2006)

The dynamics in a GaAs-type quantum dot induced by excitation with Gaussian laser pulses of arbitrary duration are calculated in the density matrix formalism using the correlation expansion. In particular the back-action of nonequilibrium phonons, i.e., the coherent phonon amplitude and the nonequilibrium phonon occupation, on the electronic two-level system are studied. We find that especially for long pulses and low temperatures nonequilibrium phonons play an important role and cannot be neglected.

DOI: 10.1103/PhysRevB.73.035302 PACS number(s): 78.67.Hc, 63.22.+m, 63.20.Kr, 03.65.Yz

I. INTRODUCTION

Semiconductor quantum dots (QDs), sometimes also called artificial atoms, combine useful properties of atoms and semiconductors. They have a discrete level structure similar to the former and provide for the possibility to be implemented into electronic devices based on semiconductor materials. Therefore they are attractive candidates for optoelectronic applications such as new types of lasers,[1] single photon sources,[2] quantum encryption devices,[3] or qubits in quantum computers.[4,5]

Most of these applications require quantum mechanical coherence, e.g., to coherently control a qubit by field-induced Rabi oscillations. One of the various conceivable realizations of a qubit is to consider the presence or absence of an exciton as the two level states. Encouragingly, Rabi oscillations of excitons have already been observed experimentally.[6–12] However, there are several mechanisms that may cause decoherence. Some of them are related to the specific experimental set up, e.g., tunnel couplings if currents in photodiodes are measured[9] or the decay to the exciton ground state if excited state Rabi oscillations are studied.[8,11,13] Other sources of setup related decoherence are inhomogeneous broadening due to the distribution of dipole moments in QD ensembles[10] or strong coupling to the radiation field for QDs created by interface fluctuations caused by their large dipole moments.[6] Further processes that lead to relaxation are radiative decay,[14–16] anharmonic phonon couplings,[17,18] charge fluctuations in the surrounding environment,[19] or off-resonant excitation of wetting layer states.[20] In this paper we will study Rabi oscillations in the exciton system focussing on decoherence and unitary corrections caused by carrier coupling to the lattice modes which may become the dominant mechanism in typical self-assembled QDs. Although phonon-mediated real transitions are suppressed in QDs due to their discrete level structure, elastic scattering with the phonons, so-called "pure dephasing," may lead to the loss of the phase relation between the levels. It thus can impede coherent control. Pure dephasing has been studied in various theoretical works[21–29] and good agreement with experiments[26] shows that it describes very well the initial dephasing after excitation by ultrashort pulses. This initial decoherence evolves on much shorter time scales than the other relaxation processes listed above. It is of exclusively quantum mechanical and non-Markovian nature. The latter manifests itself in physically interesting properties such as a non monotonous temperature dependence[26] and a nonexponential time dependence[25,26,28,30] of the initial decay, correlated to non-Lorentzian spectra.[25,29]

A full understanding of the processes going on between the carriers and the phonon system on short time scales requires insight not only into the carrier but also into the phonon dynamics. While nonequilibrium phonons have been subject to extensive studies in extended semiconductors,[31–38] to the best of our knowledge the back action of nonequilibrium phonons on the carrier dynamics in a QD has not been investigated so far. Many studies of the carrier-phonon dynamics in QDs have concentrated on ultrafast (δ pulse) excitations.[25,27–29,39] However, since in the pure dephasing model the electron density can only be affected during the pulse, it is impossible to examine how the nonequilibrium phonons, which are generated by the charge modifications in the dot, act back on the carrier dynamics in the case of a δ pulse. Whenever longer pulses have been considered the role of nonequilibrium phonons has either not been adressed[23,24] or they have been neglected.[21,22]

In this paper we will present a study on the back action of nonequilibrium phonons on the optical induced dynamics of a QD during excitation by Gaussian pulses of arbitrary length. For the coupling to phonons we will concentrate on pure dephasing processes which are described by the independent Boson model, disregarding the relaxation mechanisms that evolve on longer time scales. In the case of ultrafast excitation the coupled carrier-light carrier-phonon model even provides analytical solutions. For finite pulse durations, however, approximation schemes have to be applied. We treat the dynamics in the density matrix formalism. To truncate the infinite hierarchy of phonon-assisted density matrices we will resort to the correlation expansion[40] where we account for all single and double assisted density matrices as well as for coherent phonon amplitudes and nonequilibrium phonon occupations and correlations. Density matrices involving only phonon operators describe the nonequilibrium properties of the phonon system. By comparing calculations where these variables are set to their thermal equilibrium values with results where the full nonequilibrium dynamics is kept we can identify the influence of the nonequilibrium phonons.

 ©2006 The American Physical Society

The paper is organized as follows. In Sec. II we will introduce the dynamical variables and derive the equations of motion in the correlation expansion. After this we will briefly compare the approximative result with the exact analytical solution in the case of a δ-pulse excitation in Sec. III A. Section III B is then devoted to calculations of Rabi oscillations of the electron density. The paper ends with a summary and conclusions.

II. THEORY

We consider a QD with well separated sublevels such that we can concentrate on the optical transitions from the uppermost level in the valence band to the lowest conduction band state. Our Hamiltonian is the standard Hamiltonian for pure dephasing as already introduced in Refs. 25, 28, 29, and 41:

$$H = \hbar\Omega c^\dagger c - (\mathbf{M}\cdot\mathbf{E}^{(+)}c^\dagger d^\dagger + \mathbf{M}^*\cdot\mathbf{E}^{(-)}dc) + \sum_{\mathbf{q}}\hbar\omega_{\mathbf{q}}b_{\mathbf{q}}^\dagger b_{\mathbf{q}} + \hbar c^\dagger c\sum_{\mathbf{q}}(g_{\mathbf{q}}b_{\mathbf{q}} + \text{H.c.}). \quad (1)$$

Here the Fermi operators $c^\dagger$, $c(d^\dagger, d)$ create or annihilate an electron (hole). The gap energy $\hbar\Omega$ may also include excitonic renormalizations.[39,42] The interaction of the carriers with an external laser field is considered in dipole and rotating wave approximation and we denote the dipole matrix element by $\mathbf{M}$ and the positive (negative) frequency component of the electric field by $\mathbf{E}^{(+)}$ ($\mathbf{E}^{(-)}$). The Bose operator $b_{\mathbf{q}}^\dagger(b_{\mathbf{q}})$ creates (annihilates) a phonon with wave vector $\mathbf{q}$ and energy $\hbar\omega_{\mathbf{q}}$. We have made use of the fact that, if we start with an initially empty dot, electron and hole numbers are always equal, so that $c^\dagger c = d^\dagger d$, which allows us to write the carrier-phonon coupling in a compact form by introducing the coupling element $g_{\mathbf{q}} = g_{\mathbf{q}}^e - g_{\mathbf{q}}^h$. The matrix elements $g_{\mathbf{q}}^{e/h}$ for a spherical QD with Gaussian wave functions for the electron/hole are given explicitly in Ref. 28. We will concentrate on the deformation potential coupling to longitudinal acoustic phonons as it is known to cause the main contribution to the dephasing in typical III–V QDs without strong electron-hole separation on the time scales which will be studied here.[21,25,26,29,39] Especially the polar coupling to LO phonons in our system is very weak already in the δ pulse limit.[29] For finite pulses it will decline even more since the LO-phonon sidebands will no longer be excited by a spectrally sharper pulse. The dispersion relation of the LA phonons is assumed to be linear, $\omega_{\mathbf{q}} = c_L q$, where c_L is the longitudinal sound velocity and q denotes the modulus of the wave vector $\mathbf{q}$. Deviations from the linear dispersion are known to be of minor importance for the decoherence of typical QDs.[29] Also refinements like the assumption of more realistic carrier wave functions only lead to small quantitative deviations of the result.[39] We estimate that including confined phonon modes in dots as described, e.g., in Ref. 43 would not alter much of the results. In contrast to the case of LO phonons effects due to size quantization for the LA-phonon modes are pronounced only if the elastic properties of the embedding material differ considerably from those of the dot[44,45] which is not the case here. Within this simple model good agreement with experiments has been achieved.[26]

In our calculations the material parameters are the same as in Ref. 28, apart from the deformation potential constant $D^{e/h}$ for electrons/holes and the localization lengths of the electron/hole $a_{e/h}$. Here we use $D^e = 7.0$ eV and $D^h = -3.5$ eV as in Ref. 26; the localization length of the electron has been chosen $a_e = 3$ nm which corresponds to a full width of half maximum of the electron density of about 5 nm. The ratio $a_h/a_e = 0.87$ results from the assumption of equal potential shapes for electrons and holes.[29]

We shall use the correlation expansion within the density matrix approach to calculate the dynamical variables of the electronic subsystem. These are the electron density $f = \langle c^\dagger c\rangle$ and the interband polarization $p = \langle dc\rangle$, which is related to the complex polarization vector by $\mathbf{P} = \mathbf{M}^* p$. Due to the coupling to the phonons we will have to deal with a hierarchy of phononic and phonon-assisted density matrices.[46,47] For the phonons, since there is no number conservation, the lowest order density matrix is the coherent phonon amplitude $B_{\mathbf{q}} = g_{\mathbf{q}}\langle b_{\mathbf{q}}\rangle$. For convenience the coupling matrix element has been included in the last definition. Within the correlation expansion all higher order dynamical variables are then constructed from the respective higher order density matrices by subtracting all possible factorizations into lower order density matrices, e.g., for the two-phonon correlation

$$n_{\mathbf{q},\mathbf{q}'} = g_{\mathbf{q}}^* g_{\mathbf{q}'}\langle b_{\mathbf{q}}^\dagger b_{\mathbf{q}'}\rangle - B_{\mathbf{q}}^* B_{\mathbf{q}'} = g_{\mathbf{q}}^* g_{\mathbf{q}'}\delta\langle b_{\mathbf{q}}^\dagger b_{\mathbf{q}'}\rangle. \quad (2)$$

The equations of motion for the already introduced quantities read

$$\frac{d}{dt}f = -\frac{i}{\hbar}(\mathbf{M}^*\cdot\mathbf{E}^{(-)}p - \mathbf{M}\cdot\mathbf{E}^{(+)}p^*), \quad (3)$$

$$\frac{d}{dt}p = -i\left(\Omega + 2\sum_{\mathbf{q}}\text{Re}(B_{\mathbf{q}})\right)p + i\frac{\mathbf{M}\cdot\mathbf{E}^{(+)}}{\hbar}(1-2f) - i\sum_{\mathbf{q}}(t_{\mathbf{q}}^{(+)} + t_{\mathbf{q}}^{(-)}), \quad (4)$$

$$\frac{d}{dt}B_{\mathbf{q}} = -i\omega_{\mathbf{q}}B_{\mathbf{q}} - i|g_{\mathbf{q}}|^2 f, \quad (5)$$

$$\frac{d}{dt}n_{\mathbf{q},\mathbf{q}'} = i(\omega_{\mathbf{q}} - \omega_{\mathbf{q}'})n_{\mathbf{q},\mathbf{q}'} + i|g_{\mathbf{q}}|^2 s_{\mathbf{q}'} - i|g_{\mathbf{q}'}|^2(s_{\mathbf{q}})^*, \quad (6)$$

where $\text{Re}(\cdots)$ denotes the real part. Obviously this set of equations is not closed, but as a result of the above mentioned hierarchy problem the equations for p and $n_{\mathbf{q},\mathbf{q}'}$ contain phonon-assisted correlations

$$t_{\mathbf{q}}^{(+)} = g_{\mathbf{q}}\langle dcb_{\mathbf{q}}\rangle - pB_{\mathbf{q}} = g_{\mathbf{q}}\delta\langle dcb_{\mathbf{q}}\rangle,$$

$t_{\mathbf{q}}^{(-)} = g_{\mathbf{q}}^*\delta\langle dcb_{\mathbf{q}}^\dagger\rangle$ and $s_{\mathbf{q}} = g_{\mathbf{q}}\delta\langle c^\dagger cb_{\mathbf{q}}\rangle$. The truncation of this hierarchy is now based on the expectation that the correlations become less important with increasing number of involved particles, i.e., increasing number of operators involved in the correlation.

In the second order of the correlation expansion which is often employed for higher dimensional systems we would neglect all four-operator entities, which corresponds to the second order Born approximation. However, it turns out to be necessary for our purposes to proceed one step further in the correlation expansion.[21,22] In addition to the variables already introduced, we thus have to include the following dynamical variables: a second phonon coherence containing two phonon operators

$$n^{(+)}_{\mathbf{q},\mathbf{q}'} = g_{\mathbf{q}} g_{\mathbf{q}'} \delta\langle b_{\mathbf{q}} b_{\mathbf{q}'}\rangle$$

as well as the two-phonon assisted correlations

$$T_{\mathbf{q},\mathbf{q}'} = g^*_{\mathbf{q}} g_{\mathbf{q}'} \delta\langle dcb^\dagger_{\mathbf{q}} b_{\mathbf{q}'}\rangle, \quad S_{\mathbf{q},\mathbf{q}'} = g^*_{\mathbf{q}} g_{\mathbf{q}'} \delta\langle c^\dagger c b^\dagger_{\mathbf{q}} b_{\mathbf{q}'}\rangle,$$

$$T^{(+)}_{\mathbf{q},\mathbf{q}'} = g_{\mathbf{q}} g_{\mathbf{q}'} \delta\langle dcb_{\mathbf{q}} b_{\mathbf{q}'}\rangle, \quad S^{(+)}_{\mathbf{q},\mathbf{q}'} = g_{\mathbf{q}} g_{\mathbf{q}'} \delta\langle c^\dagger c b_{\mathbf{q}} b_{\mathbf{q}'}\rangle,$$

$$T^{(-)}_{\mathbf{q},\mathbf{q}'} = g^*_{\mathbf{q}} g^*_{\mathbf{q}'} \delta\langle dcb^\dagger_{\mathbf{q}} b^\dagger_{\mathbf{q}'}\rangle.$$

Finally there are the coherences and correlations of three phonon operators

$$N^{(+)}_{\mathbf{q},\mathbf{q}',\mathbf{q}''} = g_{\mathbf{q}} g_{\mathbf{q}'} g_{\mathbf{q}''} \delta\langle b_{\mathbf{q}} b_{\mathbf{q}'} b_{\mathbf{q}''}\rangle,$$

$$N^{(-)}_{\mathbf{q},\mathbf{q}',\mathbf{q}''} = g^*_{\mathbf{q}} g_{\mathbf{q}'} g_{\mathbf{q}''} \delta\langle b^\dagger_{\mathbf{q}} b_{\mathbf{q}'} b_{\mathbf{q}''}\rangle.$$

The remaining equations of motion are given in the appendix. In principle also the four-phonon correlations should be included. However, on the present level they do not couple back to the other variables and therefore they are not calculated. In addition we have checked that the influence of the three-phonon variables $N^{(\pm)}_{\mathbf{q},\mathbf{q}',\mathbf{q}''}$ on the carrier dynamics for all parameters used is negligible. Therefore they are not included in the calculations shown in this paper.

The system of equations of motion now is complete up to third order in the correlation expansion and without any explicit approximations made with respect to the carrier-field interaction. Thus, the light field coupling is treated nonperturbativly and all one- and two-phonon processes are included exactly. In contrast to strict perturbation theory with respect to the carrier-phonon coupling also all sequences of one- and two-phonon processes are fully included. These describe repeated one- or two-phonon scattering events (for a comparison of results obtained by applying either the correlation expansion or the perturbation theory see Ref. 41). The level of truncation applied here was also employed in the calculations in Refs. 21 and 22 where the validity of the expansion has been checked by comparison with the known analytical solution for the linear response after a δ-pulse excitation, i.e., without nonequilibrium phonons.

Our calculations always start with an unexcited electronic system and the lattice at thermal equilibrium. Initially, the only nonvanishing variable is thus $n_{\mathbf{q},\mathbf{q}'} = |g_{\mathbf{q}}|^2 n^0_q \delta_{\mathbf{q},\mathbf{q}'}$ with $n^0_q = [\exp(\hbar\omega_{\mathbf{q}}/k_B T) - 1]^{-1}$, where k_B is Boltzmann's constant. Neglecting nonequilibrium phonons then means that we keep all pure phonon variables, i.e., $B_{\mathbf{q}}$, $n_{\mathbf{q},\mathbf{q}'}$, and $n^{(+)}_{\mathbf{q},\mathbf{q}'}$, at their initial thermal values. By comparing such calculations with the full solution of the equations of motion, we can clearly identify the role of nonequilibrium phonons in the numerical results presented in the following sections. We want to remark that it makes a difference whether one leaves out the non equilibrium phonons already in the definition of the correlated dynamical variables (such that $t^{(+)}_{\mathbf{q}} = \delta\langle dcb_{\mathbf{q}}\rangle = \langle dcb_{\mathbf{q}}\rangle$) or after having setup the equations of motion. This is because the factorized parts consisting of nonequilibrium phonon variables lead to source terms in the equations of motion of other correlations and not all of these source terms vanish after setting the non equilibrium phonon variables to zero. For example the term $-ip|g_{\mathbf{q}}|^2 f$ in Eq. (A2), which stems from the equation of motion of the coherent phonon amplitude, would not be present if $B_{\mathbf{q}}$ had been neglected already in the definition of $t^{(-)}_{\mathbf{q}}$.

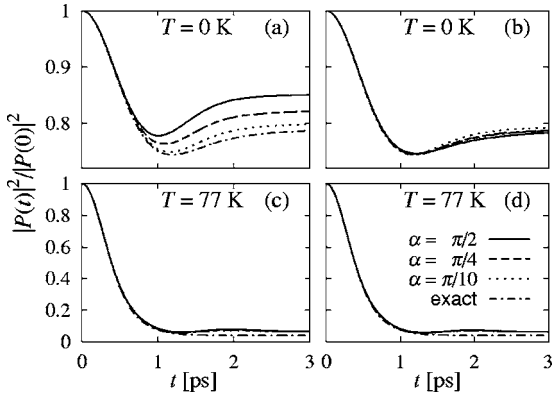

FIG. 1. Normalized polarization after a δ-pulse excitation for different rotation angles α. Left column: calculations without nonequilibrium phonons; right column: full calculations. (a) and (b) temperature $T=0$ K, (c) and (d) $T=77$ K. Solid line: $\pi/2$-pulse; dashed line: $\pi/4$-pulse; dotted line: $\pi/10$-pulse; dash-dotted line: exact result.

III. RESULTS

A. Ultrafast excitation: Comparison with exact results

In the case of excitation by a single δ-shaped pulse or a series of δ-shaped pulses the exact analytical solutions for all electronic, phononic, and phonon-assisted density matrices are known.[25] Therefore we first tested the influence of the nonequilibrium phonons by applying δ-pulse excitations and taking the exact solution as a reference. The results are shown in Fig. 1 where we have plotted the absolute square of the polarization after a δ pulse, normalized to its maximum value at $t=0$ ps, for different rotation angles, i.e., for different final electron densities, and different temperatures.

Figures 1(a) and 1(b) show the polarization at temperature $T=0$ K, in (c) and (d) the polarization is taken at $T=77$ K. In Figs. 1(b) and 1(d) nonequilibrium phonons are included whereas in Figs. 1(a) and 1(c) they are left out.

Interestingly, at low temperatures the polarization calculated without nonequilibrium phonons [Fig. 1(a)] turns out to be strongly dependent on the rotation angle. This, however, is an artifact, as the exact result for the normalized polarization (dash-dotted line) is known to be independent of the rotation angle. Including the nonequilibrium phonons [Fig.

1(b)] gives a far better approximation of the exact result. Here the dependence on the rotation angle is only very weak.

The difference between Figs. 1(a) and 1(b) is exclusively and in almost equal parts due to nonequilibrium phonon correlations and coherences, $n_{\mathbf{q},\mathbf{q}'}$ and $n^{(+)}_{\mathbf{q},\mathbf{q}'}$, whereas the coherent phonon amplitude $B_{\mathbf{q}}$ does not play any role for the polarization after a δ pulse excitation. In the following it will not be necessary to distinguish between $n_{\mathbf{q},\mathbf{q}'}$ and $n^{(+)}_{\mathbf{q},\mathbf{q}'}$ and we will refer to both entities as nonequilibrium occupations.

At higher temperatures the difference between the right and the left column disappears. The effect of the nonequilibrium phonons has been washed out by thermal phonons. Thus, we have seen that indeed on the present level the correlation expansion agrees well with the exact results. However, at low temperatures it is essential to include nonequilibrium phonons. This holds even for weaker electron-phonon coupling (larger QDs) which does not change the results shown in Fig. 1 in a qualitative way.

It turns out that also for finite pulse durations nonequilibrium phonons are less important at $T=77$ K. Therefore, in the following we will restrict ourselves to the case of low temperatures, i.e., $T=0$ K.

B. Rabi oscillations

While the exact solution for the dynamical variables is only known for δ-pulse excitations, the correlation expansion provides the possibility to study also pulses of longer duration. Here we will model the light field by Gaussian laser pulses

$$\mathbf{E}^{(+)}(t) = \mathbf{E}^{(-)*}(t) = \tilde{\mathbf{E}}(t)e^{-i\omega t}, \tag{7}$$

$$\tilde{\mathbf{E}}(t) = \mathbf{E}_0 \exp\left\{-\frac{1}{2}\left(\frac{t}{\tau_0}\right)^2\right\}. \tag{8}$$

In the following the laser pulses will be characterized by their full width at half maximum of the intensity τ, which is related to τ_0 by $\tau = 2\sqrt{\ln 2}\,\tau_0$.

Again we will analyze the differences between calculations including nonequilibrium phonons and those without them. But in this section we will concentrate on their effect on the electron density f.

In Fig. 2 we have plotted the real time dynamics of the electron density during an $\alpha = 4\pi$-pulse of duration $\tau = 1$ ps, where α is defined as the nominal rotation angle

$$\alpha = \frac{2}{\hbar}\int_{-\infty}^{\infty} dt' \mathbf{M}\cdot\tilde{\mathbf{E}}(t'). \tag{9}$$

The solid lines show the results obtained where nonequilibrium phonons were included, the dashed lines those where they were left out. The dotted lines refer to a calculation without carrier-phonon coupling. In Fig. 2(a) the central laser frequency has been chosen to be

$$\omega = \bar{\Omega} = \Omega - \sum_{\mathbf{q}} \frac{|g_{\mathbf{q}}|^2}{\omega_{\mathbf{q}}}, \tag{10}$$

i.e., the polaron shifted transition frequency, whereas Fig. 2(b) shows the dynamics during a pulse of central frequency

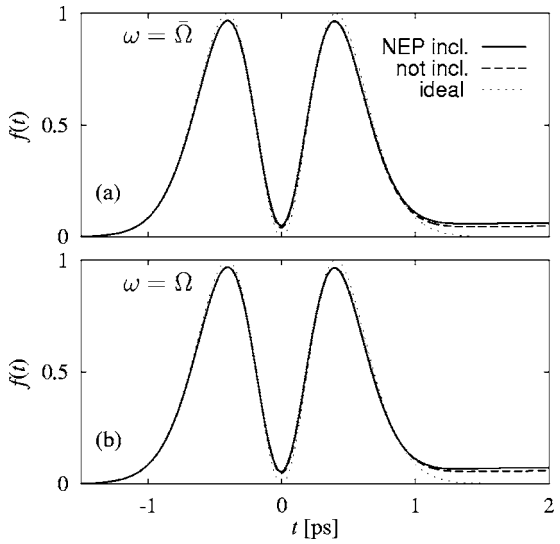

FIG. 2. Rabi oscillation during a nominal 4π pulse with $\tau = 1$ ps at temperature $T=0$ K. (a) Excitation at $\omega=\bar{\Omega}$; (b) excitation at $\omega=\Omega$. Solid line: nonequilibrium phonons (NEP) included; dashed line: without nonequilibrium phonons; dotted line: ideal Rabi oscillations for resonant excitation without phonon coupling.

$\omega=\Omega$, i.e., at the bare electron (exciton) energy. The polaron shifted frequency $\bar{\Omega}$ determines the position of the resonance in the linear absorption, while Ω indicates where this resonance would be if it were possible to switch off the carrier-phonon interaction.

Without the coupling to the phonon system, the electron occupation undergoes a perfect 4π rotation (dotted line). However, the interaction with the lattice modes induces a dephasing and thus inhibits a fully coherent control, so the density cannot be driven back to the initial value zero. The comparison in Fig. 2(a) shows that the amount of the phonon induced decoherence is only very slightly increased by including nonequilibrium phonons in the calculation. The additional dephasing again is due to the nonequilibrium phonon occupations, while the coherent phonon amplitudes do not produce any effect.

Figure 2(b), where the excitation has been tuned to the bare electron energy Ω, shows almost the same result as Fig. 2(a). For the present case of a 1 ps pulse this has to be expected since its spectral width is larger than the small polaron shift of $\hbar(\Omega-\bar{\Omega})\approx 0.18$ meV.

But let us now come to longer pulses. Figure 3 shows the real time dynamics of the electron occupation during a $\tau = 12$ ps pulse. Again in Fig. 3(a) the laser frequency is $\omega = \bar{\Omega}$ and in (b) the system is excited with $\omega=\Omega$. Now there are clearly visible differences. In the upper figure the Rabi rotations including nonequilibrium phonons (solid line) are typical of a resonant excitation. During the first Rabi flop the electron occupation comes even closer to the values zero and one than during the 1 ps pulse. An explanation for this is that because of the slower charge modification the lattice can follow almost adiabatically whereas a pulse duration of 1 ps is close to the characteristic time scale of the phonon dynamics,[24] which is about a few picoseconds, and so the

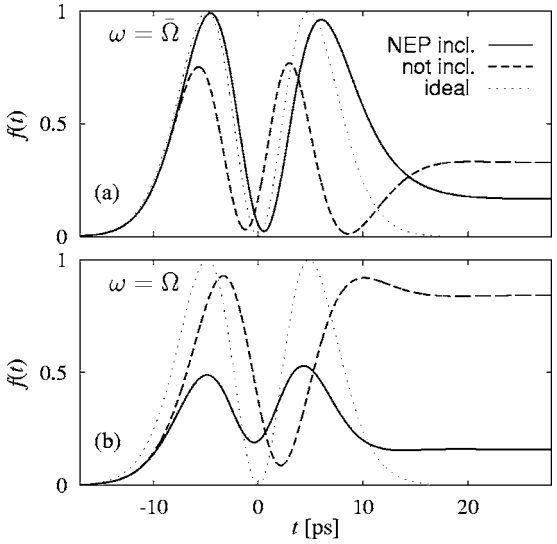

FIG. 3. Rabi oscillation during a nominal 4π pulse with $\tau = 12$ ps at temperature $T=0$ K. (a) Excitation at $\omega=\bar{\Omega}$; (b) excitation at $\omega=\Omega$. Solid line: nonequilibrium (NEP) phonons included; dashed line: without nonequilibrium phonons; dotted line: ideal Rabi oscillations for resonant excitation without phonon coupling.

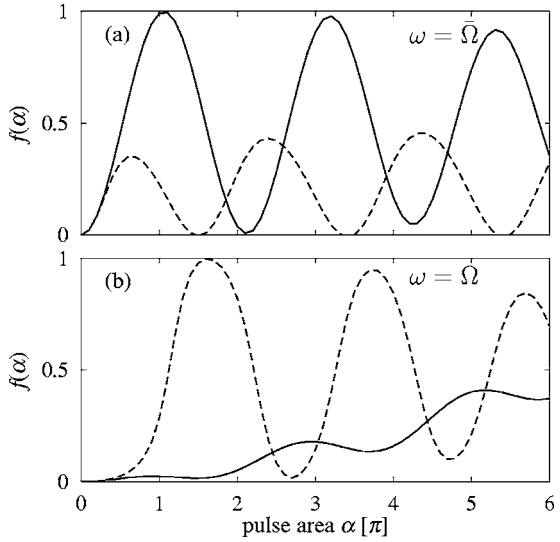

FIG. 4. Occupation of the upper level vs pulse area after a $\tau = 12$ ps pulse at $T=0$ K. (a) Excitation at $\omega=\bar{\Omega}$; (b) excitation at $\omega=\Omega$. Solid line: nonequilibrium phonons included; dashed line: without nonequilibrium phonons.

interaction is enhanced. It should be noticed that although α has been chosen to be 4π, the electron occupation seems to perform a rotation of an effective angle $\alpha_{\text{eff}} \leqslant \alpha$. Such a deviation from the nominal rotation angle is already known from earlier studies,[21,23,41] where it was found to be intensity dependent.

The calculation without nonequilibrium phonons (dashed line) exhibits diminished amplitudes, however, the system here also seems to suffer only little decoherence since the amplitudes do not decrease. Furthermore we observe that the Rabi frequency is increased in comparison to the nominal one, as the occupation seems to undergo a 4.5π rotation. Such behavior would have been expected for off-resonant excitation. In particular, for the case of monochromatic excitation of an isolated two-level-system it is possible to give an explicit formula for the electron density. Assuming $f(0)=0$ it reads[48]

$$f(t) = \frac{\Omega_R^2}{\tilde{\Omega}^2} \sin^2 \tilde{\Omega} t \tag{11}$$

with $\Omega_R = \mathbf{M}\cdot\tilde{\mathbf{E}}/\hbar$ and

$$\tilde{\Omega} = \sqrt{\Omega_R^2 + \left(\frac{\delta\omega}{2}\right)^2}, \tag{12}$$

where $\delta\omega$ is the deviation from the resonance frequency. Obviously, Eq. (11) predicts a shift of the Rabi frequency given by Eq. (12) as well as a reduction of the amplitude of the rotations, similar to what we find numerically in Fig. 3(a).

Figure 3(b) looks quite complementary to Fig. 3(a), where the laser frequency is $\omega=\Omega$. Here, the full calculation with nonequilibrium phonons (solid line) only leads to off resonant Rabi oscillations of reduced amplitude but increased Rabi frequency $\bar{\Omega}$ [compared to Fig. 3(a)]. In addition the curve is slightly shifted upwards. This can be explained by the fact that above the frequency $\bar{\Omega}$ there is a continuum of possible phonon-assisted excitations.

The curve calculated without nonequilibrium phonons (dashed line), on the other hand, seems to be much better in resonance as the density nearly reaches the value one. The rotation angle, however, is effectively only about 3π instead of the nominal value 4π. The different resonance behavior for calculations with or without nonequilibrium phonons is surprising, because the polaron shift is already inherent in the linear absorption spectrum where the nonequilibrium phonons do not enter. Therefore in both calculations the linear absorption has its resonance at the phonon shifted frequency $\bar{\Omega}$.

To see the effect of the intensity-dependent rotation angle more clearly, and also because it is experimentally better accessible, we show in Fig. 4 the final electron occupation after a 12 ps pulse as a function of the nominal pulse area α, again for the two different excitation frequencies. In Fig. 4(a) the occupation calculated with nonequilibrium phonons included exhibits rather good Rabi oscillations, although with increasing pulse area a stronger decoherence becomes visible. Also the extrema deviate increasingly from their nominal positions at integer multiples of π which confirms again that α_{eff} is intensity dependent.

The graph looks totally different calculated without nonequilibrium phonons. Here the amplitudes of the oscillations do not exceed the value 0.5 and, although the system is excited at the linear absorption energy, the Rabi frequency is evidently increased as it would be expected for off-resonant excitation. Note that for higher field intensity the occupation number even reaches unphysical negative values at the minima, which is a clear indication of the inconsistency of the model if nonequilibrium phonons are neglected. A similar

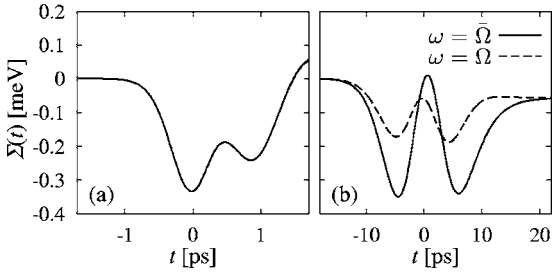

FIG. 5. Real-time dynamics of Σ for excitation with $\omega=\bar{\Omega}$ (solid line) and $\omega=\Omega$ (dashed line): (a) $\tau=1.0$ ps, (b) $\tau=12.0$ ps at temperature $T=0$ K.

unphysical behavior has been reported for calculations involving a single optical phonon mode when nonequilibrium phonons were neglected.[49]

In Fig. 4(b), where the excitation frequency is $\omega=\Omega$, the calculation without nonequilibrium phonons seems to undergo resonant Rabi oscillations, since the occupation reaches the value one, though the rotation angle is considerably shifted. In contrast, the full calculation exhibits clearly an off resonant behavior. The amplitude of the oscillations is strongly reduced and for stronger fields there is a significant electron density due to phonon assisted excitation.

Let us now take a look at the equations of motion to see where the differences might stem from. We notice that the coherent phonon amplitudes only occur in combination with the bare gap energy Ω. Namely, in the homogeneous part of Eq. (4) and all other equations of motion for phonon assisted density matrices containing the operator dc. In these terms the sum over the real parts of the coherent phonon amplitudes $(1/\hbar)\Sigma=2\Sigma_{\mathbf{q}}\mathrm{Re}(B_{\mathbf{q}})$ modifies Ω in an electron density and time dependent manner. Physically the coherent phonon amplitudes can be related to a relative volume change[27] which is experimentally observable.[50]

Figure 5 shows the real-time dynamics of Σ for a pulse duration of 1 ps (a) and for 12 ps (b). From Eq. (5) it is clear that the coherent amplitudes follow the electron occupation similar to a driven harmonic oscillator, only with the opposite sign. But as the laser pulse in Fig. 5(a) is short compared to the characteristic times of the phonon coupling, the dynamics are retarded with respect to f. The minima are not distributed symmetrically around $t=0$ ps, but they are delayed by about half a picosecond and they are of different heights. This retardation reflects that the phonon system has a memory which turns the phonon expectation values on these time scales into independent variables. For the long pulse in Fig. 5(b), however, this delay is negligible and Σ reflects almost exactly the electron dynamics. The coherent phonon amplitudes thus seem to compensate the effect of the charge modification on the transition frequency and to keep it stable at the polaron shift, in contrast to the calculation without nonequilibrium phonons. From Eqs. (5) and (10) we estimate that in the adiabatic limit for integer multiples of $\alpha=2\pi$ and resonant excitation, where the average electron density is one half, the average of Σ should be given by the polaron shift $\hbar(\bar{\Omega}-\Omega)$ (here about 0.18 meV) which agrees pretty well with the average value of the solid line in Fig. 5(b).

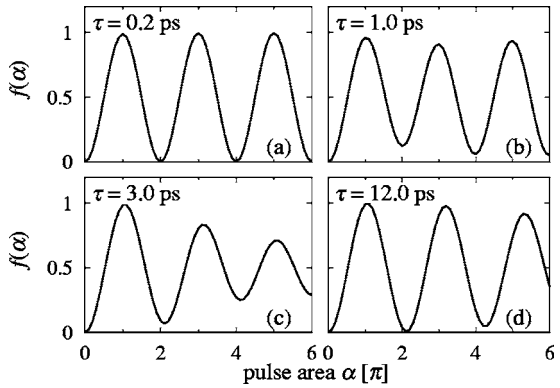

FIG. 6. Occupation of the upper level vs pulse area for different pulse lengths after an excitation at $\omega=\bar{\Omega}$ for temperature $T=0$ K.

For long pulses mainly the coherent phonon amplitude turns out to be responsible for the different results for calculations with or without nonequilibrium phonons. In this limit the nonequilibrium phonon occupations are almost negligible. On the contrary, for short pulses the coherent phonon amplitudes do not play a role, as already stated before, since they exclusively contribute to the transition frequency. The resulting changes of the resonance, however, can only be resolved in the case of sufficiently long pulses corresponding to sharp pulse spectra.

For larger QDs the effects due to the coherent phonon amplitudes are much less pronounced for the pulse durations we are here dealing with, though still clearly perceptible at least at low temperatures. This reflects the weaker carrier-phonon coupling strength for larger dots. It would thus need longer pulses to spectrally distinguish the energies $\hbar\bar{\Omega}$ and $\hbar\Omega$ and see the effects as clearly as for a 3 nm QD.

Figure 6 shows Rabi oscillations as a function of the nominal pulse area α for excitation with four different pulse durations at the correct transition frequency $\omega=\bar{\Omega}$. For a very short pulse [0.2 ps in Fig. 6(a)] we find almost perfect oscillations since the pulse duration is too short for the phonon system to react and after the pulse the occupation cannot be changed anymore. Intermediate pulse lengths [1.0 and 3.0 ps in Figs. 6(b) and 6(c)] lead to increased decoherence as these durations are in the range of the phonon-induced time scales. By enlarging the pulse duration [12 ps in Fig. 6(d)] the quality of the oscillation gets better again, because the phonon system is now able to follow the carrier dynamics adiabatically. This nonmonotonous dependence on the pulse duration reflects the non-Markovian character of the carrier-phonon interaction. Similar results were also found in Refs. 21 and 22. The calculations there were done for larger dots and at $T=77$ K. In agreement with our findings the authors have noted that nonequilibrium phonons are of minor importance for the cases studied there. However, this does not hold for lower temperatures.

It is instructive to take a look at the total number of phonons [see Eq. (2)]

$$N=\sum_{\mathbf{q}}\langle b_{\mathbf{q}}^{\dagger}b_{\mathbf{q}}\rangle=\sum_{\mathbf{q}}\frac{1}{|g_{\mathbf{q}}|^2}(n_{\mathbf{q},\mathbf{q}}+|B_{\mathbf{q}}|^2).$$

We have plotted N in Fig. 7 as a function of the rotation angle α for times long after the pulse so that f and p have

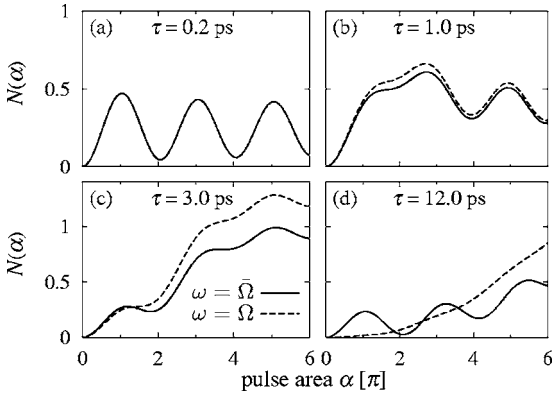

FIG. 7. Total phonon number vs pulse area for different pulse lengths after excitation at $\omega=\bar{\Omega}$ (solid lines) and excitation at $\omega=\Omega$ (dashed lines) for temperature $T=0$ K and $t\to\infty$.

reached their final value. The solid lines refer to the excitation at $\omega=\bar{\Omega}$ whereas excitation with $\omega=\Omega$ is plotted with dashed lines. The pulse durations are the same as in Fig. 6. There is a clear correlation between the quality of the Rabi oscillations in Fig. 6 and the behavior of the corresponding total phonon number (solid lines). The short pulse limit in Fig. 7(a) can be understood by the analytical results obtained for δ-pulse excitation:[25] the number of generated phonons is strictly related to the electron density and therefore exhibits nearly perfect oscillations; one half of the generated phonons stays in the dot region and builds up the polaron complex, the other half leaves the dot in form of a phonon wave packet. Of course, these dynamics cannot have any impact on the electron occupation, because the phonons are generated after the pulse when f can no longer be changed by pure dephasing processes. We would like to remark that emission of phonon wave packets from optically excited quantum dots has already been observed in bolometric experiments.[51,52] In Fig. 7(b), i.e., for $\tau=1$ ps, where the corresponding electron occupation already suffers some decoherence, we see that the total phonon number first takes the same rise as in (a). But while for a delta pulse the phonon generation must be symmetric around $\alpha=\pi$, for longer pulses memory processes come into play so there is phonon production during and after the charge rotation. The phonons that are not involved in the building of the polaron leave the dot and cannot be removed anymore.[25,39,53]

Similar to Fig. 7(b) we observe in Fig. 7(c) that the phonon production is no longer strictly related to the electron dynamics due to memory effects and the generation of leaving wave packets. The phononic expectation values become independent variables. However, for the 3 ps pulse the increase of the total phonon number with the pulse area is first weaker and then stronger than for the 1 ps pulse. Furthermore we note that the system is more frequency selective. The difference between excitation at $\omega=\bar{\Omega}$ (solid line) and excitation at $\omega=\Omega$ (dashed line) is much more pronounced than in Fig. 7(b). In both situations the off-resonant excitation at $\omega=\Omega\geqslant\bar{\Omega}$ (dashed line) leads to phonon assisted excitations and thus to an enhanced phonon generation.

In the case of the $\tau=12$ ps pulse in Fig. 7(d) the maximum value for excitation at $\omega=\bar{\Omega}$ (solid line) is only half the maximum value from Fig. 7(a) indicating adiabatic dynamics where only the polaron is built up. Similar to the polaron the total phonon number exhibits oscillatory dependence on the pulse area. For excitation at $\omega=\Omega$, however, the shape rather resembles a parabola, i.e., it is essentially proportional to the total pulse intensity. Here the excitation energy lies in the continuum of the phonon sideband and the phonons are created in the phonon-assisted optical transition.

IV. SUMMARY AND CONCLUSIONS

In this work we have presented a study on the back action of nonequilibrium phonons, i.e., the nonequilibrium correlations and coherences and the coherent phonon amplitudes, on the carrier dynamics in a GaAs quantum dot for excitation by a Gaussian laser pulse of arbitrary duration. The role of these nonequilibrium phonons in the case of excitation with pulses of finite duration has not been addressed previously. Working in the density matrix formalism we employed the correlation expansion to truncate the hierarchy of density matrices in a systematic manner. By comparison with the exact analytical result known for δ-pulse excitation we determined the required level of truncation. It turned out that for low temperatures it is vital to include the nonequilibrium phonons, because neglecting the nonequilibrium phonon occupation leads to an artificial dependence on the pulse area. For elevated temperatures, however, thermal phonons dominate the phonon occupations and therefore this effect is washed out and the difference between the calculations with or without the nonequilibrium phonons vanishes.

For finite pulses we studied the influence of the nonequilibrium phonons on the dynamics of the electron density. The nonequilibrium phonon occupations mainly contribute to the relaxation dynamics of the polarization after the pulse, when processes of pure dephasing cannot change the electron occupation anymore. Thus they have only a minor impact on the electron density. The coherent phonon amplitudes enter the equations of motion only as a renormalization of the transition frequency. Therefore in the case of short laser pulses their impact can hardly be seen. However, with increasing pulse duration and hence increasing spectral sharpness the role of the coherent phonon amplitudes becomes important. It stabilizes the position of the transition energy at the polaron shift by following the dynamics of the charge density during the Rabi oscillations. Calculations without nonequilibrium phonons, in particular without coherent phonon amplitudes, exhibit off resonant behavior for excitation at the polaron shifted frequency. This is clearly unphysical, since the polaron shift constitutes the resonance in the linear absorption spectrum and thus the excitation is in resonance. In addition even unphysical negative values are reached. The full calculation, in contrast, shows neither the latter incorrect features nor such a strong density dependence of the polarization for δ-pulse excitation [Fig. 1(b)], but provides sensible results over a wide parameter range with respect to the dot size as well as to temperature.

These findings underline that in general it is inconsistent and therefore not justified to disregard the nonequilibrium phonons in the systematic correlation expansion, though for

larger QDs and higher temperatures these deviations from the full calculation may be less pronounced and sometimes even negligible.[21,22] In addition, the study of the purely phononic density matrices gives an interesting insight into how the lattice acts back on the carrier dynamics.

ACKNOWLEDGMENTS

We are grateful to P. Machnikowski and A. Vagov for fruitful discussions. This work was supported by the Deutsche Forschungsgemeinschaft.

APPENDIX A: EQUATIONS OF MOTION

For completeness we show here all the equations of motion which are not given explicitly in Sec. II. For the phonon assisted density matrices we have

$$\frac{d}{dt}t_{\mathbf{q}}^{(+)} = -i\left(\Omega+\omega_{\mathbf{q}}+2\sum_{\mathbf{q}'}\mathrm{Re}(B_{\mathbf{q}'})\right)t_{\mathbf{q}}^{(+)} - ip\Bigg[|g_{\mathbf{q}}|^2(1-f) + \sum_{\mathbf{q}'}(n_{\mathbf{q},\mathbf{q}'}^{(+)}+n_{\mathbf{q}',\mathbf{q}})\Bigg] - i\sum_{\mathbf{q}'}(T_{\mathbf{q},\mathbf{q}'}^{(+)}+T_{\mathbf{q}',\mathbf{q}}) - 2i\frac{\mathbf{M}\cdot\mathbf{E}^{(+)}}{\hbar}s_{\mathbf{q}}, \tag{A1}$$

$$\frac{d}{dt}t_{\mathbf{q}}^{(-)} = -i\left(\Omega-\omega_{\mathbf{q}}+2\sum_{\mathbf{q}'}\mathrm{Re}(B_{\mathbf{q}'})\right)t_{\mathbf{q}}^{(-)} - ip\Bigg[|g_{\mathbf{q}}|^2 f + \sum_{\mathbf{q}'}g_{\mathbf{q}'}[n_{\mathbf{q},\mathbf{q}'}+(n_{\mathbf{q},\mathbf{q}'}^{(+)})^*]\Bigg] - i\sum_{\mathbf{q}'}(T_{\mathbf{q},\mathbf{q}'}+T_{\mathbf{q},\mathbf{q}'}^{(-)}) - 2i\frac{\mathbf{M}\cdot\mathbf{E}^{(+)}}{\hbar}s_{\mathbf{q}}^*, \tag{A2}$$

$$\frac{d}{dt}s_{\mathbf{q}} = -i\omega_{\mathbf{q}}s_{\mathbf{q}} - i\frac{\mathbf{M}}{\hbar}[\mathbf{E}^{(-)}t_{\mathbf{q}}^{(+)} - \mathbf{E}^{(+)}(t_{\mathbf{q}}^{(-)})^*] - i|g_{\mathbf{q}}|^2 f(1-f). \tag{A3}$$

The equation of motion for the two-phonon correlation $n_{\mathbf{q},\mathbf{q}'}^{(+)}$ reads

$$\frac{d}{dt}n_{\mathbf{q},\mathbf{q}'}^{(+)} = -i(\omega_{\mathbf{q}}+\omega_{\mathbf{q}'})n_{\mathbf{q},\mathbf{q}'}^{(+)} - i|g_{\mathbf{q}}|^2 s_{\mathbf{q}'} - i|g_{\mathbf{q}'}|^2 s_{\mathbf{q}}. \tag{A4}$$

Furthermore we have the equations of motion for the two-phonon assisted correlations $T_{\mathbf{q},\mathbf{q}'}$, $T_{\mathbf{q},\mathbf{q}'}^{(+)}$, $T_{\mathbf{q},\mathbf{q}'}^{(-)}$, $S_{\mathbf{q},\mathbf{q}'}$, and $S_{\mathbf{q},\mathbf{q}'}^{(+)}$ which are given by

$$\frac{d}{dt}T_{\mathbf{q},\mathbf{q}'} = -i\left(\Omega-\omega_{\mathbf{q}}+\omega_{\mathbf{q}'}+2\sum_{\mathbf{q}''}\mathrm{Re}(B_{\mathbf{q}''})\right)T_{\mathbf{q},\mathbf{q}'} - i\left[|g_{\mathbf{q}'}|^2(1-f)+\sum_{\mathbf{q}''}[n_{\mathbf{q}',\mathbf{q}''}^{(+)}+n_{\mathbf{q}'',\mathbf{q}'}]\right]t_{\mathbf{q}}^{(-)} - i\left[|g_{\mathbf{q}}|^2 f+\sum_{\mathbf{q}''}[n_{\mathbf{q},\mathbf{q}''}+(n_{\mathbf{q},\mathbf{q}''}^{(+)})^*]\right]t_{\mathbf{q}'}^{(+)} - 2i\frac{\mathbf{M}\cdot\mathbf{E}^{(+)}}{\hbar}S_{\mathbf{q},\mathbf{q}'} + i[|g_{\mathbf{q}'}|^2(s_{\mathbf{q}})^* - |g_{\mathbf{q}}|^2 s_{\mathbf{q}'}]p - ip\sum_{\mathbf{q}''}[N_{\mathbf{q},\mathbf{q}',\mathbf{q}''}^{(-)}+(N_{\mathbf{q}',\mathbf{q},\mathbf{q}''}^{(-)})^*], \tag{A5}$$

$$\frac{d}{dt}T_{\mathbf{q},\mathbf{q}'}^{(+)} = -i\left(\Omega+\omega_{\mathbf{q}}+\omega_{\mathbf{q}'}+2\sum_{\mathbf{q}''}\mathrm{Re}(B_{\mathbf{q}''})\right)T_{\mathbf{q},\mathbf{q}'}^{(+)} - i\left[|g_{\mathbf{q}'}|^2(1-f)+\sum_{\mathbf{q}''}(n_{\mathbf{q}',\mathbf{q}''}^{(+)}+n_{\mathbf{q}'',\mathbf{q}'})\right]t_{\mathbf{q}}^{(+)} - i\Bigg[|g_{\mathbf{q}}|^2(1-f)+\sum_{\mathbf{q}''}(n_{\mathbf{q},\mathbf{q}''}^{(+)}+n_{\mathbf{q}'',\mathbf{q}})\Bigg]t_{\mathbf{q}'}^{(+)} - 2i\frac{\mathbf{M}\cdot\mathbf{E}^{(+)}}{\hbar}S_{\mathbf{q},\mathbf{q}'}^{(+)} + i[|g_{\mathbf{q}'}|^2 s_{\mathbf{q}}+|g_{\mathbf{q}}|^2 s_{\mathbf{q}'}]p - ip\sum_{\mathbf{q}''}(N_{\mathbf{q},\mathbf{q}',\mathbf{q}''}^{(+)}+N_{\mathbf{q}'',\mathbf{q},\mathbf{q}'}^{(-)}), \tag{A6}$$

$$\frac{d}{dt}T_{\mathbf{q},\mathbf{q}'}^{(-)} = -i\left(\Omega-\omega_{\mathbf{q}}-\omega_{\mathbf{q}'}+2\sum_{\mathbf{q}''}\mathrm{Re}(B_{\mathbf{q}''})\right)T_{\mathbf{q},\mathbf{q}'}^{(-)} - i\left[|g_{\mathbf{q}'}|^2 f+\sum_{\mathbf{q}''}[n_{\mathbf{q}',\mathbf{q}''}+(n_{\mathbf{q}'',\mathbf{q}'}^{(+)})^*]\right]t_{\mathbf{q}}^{(-)} - i\left[|g_{\mathbf{q}}|^2 f+\sum_{\mathbf{q}''}[n_{\mathbf{q},\mathbf{q}''}+(n_{\mathbf{q}'',\mathbf{q}}^{(+)})^*]\right]t_{\mathbf{q}'}^{(-)} - 2i\frac{\mathbf{M}\cdot\mathbf{E}^{(+)}}{\hbar}(S_{\mathbf{q},\mathbf{q}'}^{(+)})^* - i[|g_{\mathbf{q}'}|^2(s_{\mathbf{q}})^* + |g_{\mathbf{q}}|^2(s_{\mathbf{q}'})^*]p - ip\sum_{\mathbf{q}''}[(N_{\mathbf{q}'',\mathbf{q}',\mathbf{q}}^{(-)})^* + (N_{\mathbf{q},\mathbf{q}',\mathbf{q}''}^{(+)})^*], \tag{A7}$$

and finally

$$\frac{d}{dt}S_{\mathbf{q},\mathbf{q}'} = i(\omega_{\mathbf{q}}-\omega_{\mathbf{q}'})S_{\mathbf{q},\mathbf{q}'} - i\frac{\mathbf{M}}{\hbar}[\mathbf{E}^{(-)}T_{\mathbf{q},\mathbf{q}'} - (T_{\mathbf{q}',\mathbf{q}})^*\mathbf{E}^{(+)}] + i(1-2f)[|g_{\mathbf{q}}|^2 s_{\mathbf{q}'} - |g_{\mathbf{q}'}|^2(s_{\mathbf{q}})^*], \tag{A8}$$

$$\frac{d}{dt}S_{\mathbf{q},\mathbf{q}'}^{(+)} = -i(\omega_{\mathbf{q}}+\omega_{\mathbf{q}'})S_{\mathbf{q},\mathbf{q}'}^{(+)} - i\frac{\mathbf{M}}{\hbar}[\mathbf{E}^{(-)}T_{\mathbf{q},\mathbf{q}'}^{(+)} - (T_{\mathbf{q}',\mathbf{q}}^{(-)})^*\mathbf{E}^{(+)}] - i(1-2f)[|g_{\mathbf{q}}|^2 s_{\mathbf{q}'} + |g_{\mathbf{q}'}|^2 s_{\mathbf{q}}]. \tag{A9}$$

[1] D. Bimberg, M. Grundmann, and N. N. Ledentsov, *Quantum Dot Heterostructures* (John Wiley and Sons, Chichester, 1998).
[2] P. Michler, A. Kiraz, C. Becher, W. V. Schoenfeld, P. Petroff, L. D. Zhang, E. Hu, and A. Imamoglu, Science **290**, 2282 (2000).
[3] R. M. Stevenson, R. M. Thompson, A. J. Shields, I. Farrer, B. E. Kardynal, D. A. Ritchie, and M. Pepper, Phys. Rev. B **66**, 081302(R) (2002).
[4] E. Biolatti, R. C. Iotti, P. Zanardi, and F. Rossi, Phys. Rev. Lett. **85**, 5647 (2000).
[5] X. Q. Li, Y. W. Wu, D. Steel, D. Gammon, T. H. Stievater, D. S. Katzer, D. Park, C. Piermarocchi, and L. J. Sham, Science **301**, 809 (2003).
[6] T. H. Stievater, X. Li, D. G. Steel, D. Gammon, D. S. Katzer, D. Park, C. Piermarocchi, and L. J. Sham, Phys. Rev. Lett. **87**, 133603 (2001).
[7] H. Kamada, H. Gotoh, J. Temmyo, T. Takagahara, and H. Ando, Phys. Rev. Lett. **87**, 246401 (2001).
[8] H. Htoon, T. Takagahara, D. Kulik, O. Baklenov, A. L. Holmes, and C. K. Shih, Phys. Rev. Lett. **88**, 087401 (2002).
[9] A. Zrenner, E. Beham, S. Stufler, F. Findeis, M. Bichler, and G. Abstreiter, Nature (London) **418**, 612 (2002).
[10] P. Borri, W. Langbein, S. Schneider, U. Woggon, R. L. Sellin, D. Ouyang, and D. Bimberg, Phys. Rev. B **66**, 081306(R) (2002).
[11] L. Besombes, J. J. Baumberg, and J. Motohisa, Phys. Rev. Lett. **90**, 257402 (2003).
[12] T. Unold, K. Mueller, C. Lienau, T. Elsaesser, and A. D. Wieck, Phys. Rev. Lett. **94**, 137404 (2005).
[13] Q. Q. Wang, A. Muller, P. Bianucci, E. Rossi, Q. K. Xue, T. Takagahara, C. Piermarocchi, A. H. MacDonald, and C. K. Shih, Phys. Rev. B **72**, 035306 (2005).
[14] M. Bayer and A. Forchel, Phys. Rev. B **65**, 041308(R) (2002).
[15] W. Langbein, P. Borri, U. Woggon, V. Stavarache, D. Reuter, and A. D. Wieck, Phys. Rev. B **70**, 033301 (2004).
[16] G. Bacher, R. Weigand, J. Seufert, V. D. Kulakovskii, N. A. Gippius, A. Forchel, K. Leonardi, and D. Hommel, Phys. Rev. Lett. **83**, 4417 (1999).
[17] L. Jacak, J. Krasnyj, D. Jacak, and P. Machnikowski, Phys. Rev. B **65**, 113305 (2002).
[18] E. A. Muljarov and R. Zimmermann, Phys. Rev. Lett. **93**, 237401 (2004).
[19] T. Itakura and Y. Tokura, Phys. Rev. B **67**, 195320 (2003).
[20] J. M. Villas-Bôas, S. E. Ulloa, and A. O. Govorov, Phys. Rev. Lett. **94**, 057404 (2005).
[21] J. Förstner, C. Weber, J. Danckwerts, and A. Knorr, Phys. Rev. Lett. **91**, 127401 (2003).
[22] J. Förstner, C. Weber, J. Danckwerts, and A. Knorr, Phys. Status Solidi B **238**, 419 (2003).
[23] P. Machnikowski and L. Jacak, Phys. Rev. B **69**, 193302 (2004).
[24] P. Machnikowski and L. Jacak, Semicond. Sci. Technol. **19**, 299 (2004).
[25] A. Vagov, V. M. Axt, and T. Kuhn, Phys. Rev. B **66**, 165312 (2002).
[26] A. Vagov, V. M. Axt, T. Kuhn, W. Langbein, P. Borri, and U. Woggon, Phys. Rev. B **70**, 201305(R) (2004).
[27] A. Vagov, V. M. Axt, and T. Kuhn, Physica E (Amsterdam) **17**, 11 (2003).
[28] A. Vagov, V. M. Axt, and T. Kuhn, Phys. Rev. B **67**, 115338 (2003).
[29] B. Krummheuer, V. M. Axt, and T. Kuhn, Phys. Rev. B **65**, 195313 (2002).
[30] P. Borri, W. Langbein, S. Schneider, U. Woggon, R. L. Sellin, D. Ouyang, and D. Bimberg, Phys. Rev. Lett. **87**, 157401 (2001).
[31] L. Rota, F. Rossi, P. Lugli, and E. Molinari, Phys. Rev. B **52**, 5183 (1995).
[32] T. Dekorsy, G. Cho, and H. Kurz, in *Light Scattering in Solids VIII: Fullerenes, Semiconductor Surfaces, Coherent Phonons*, edited by M. Cardona and G. Güntherodt, Vol. 76 of *Topics in Applied Physics* (Springer, Berlin, 2000), pp. 169–209.
[33] A. V. Kuznetsov and C. J. Stanton, Phys. Rev. Lett. **73**, 3243 (1994).
[34] U. Hohenester, P. Supancic, P. Kocevar, X. Q. Zhou, W. Kütt, and H. Kurz, Phys. Rev. B **47**, 13233 (1993).
[35] A. V. Akimov, Physica B **263**, 175 (1999).
[36] P. Langot, N. Del Fatti, D. Christofilos, R. Tommasi, and F. Vallée, Phys. Rev. B **54**, 14487 (1996).
[37] E. Binder, J. Schilp, and T. Kuhn, Phys. Status Solidi B **206**, 227 (1998).
[38] M. Herbst, M. Glanemann, V. M. Axt, and T. Kuhn, Phys. Rev. B **67**, 195305 (2003).
[39] B. Krummheuer, V. M. Axt, T. Kuhn, I. D'Amico, and F. Rossi, Phys. Rev. B **71**, 235329 (2005).
[40] F. Rossi and T. Kuhn, Rev. Mod. Phys. **74**, 895 (2002).
[41] A. Krügel, V. M. Axt, T. Kuhn, P. Machnikowski, and A. Vagov, Appl. Phys. B: Lasers Opt. **81**, 897 (2005).
[42] S. Schmitt-Rink, D. A. B. Miller, and D. S. Chemla, Phys. Rev. B **35**, 8113 (1987).
[43] M. A. Stroscio and M. Dutta, *Phonons in Nanostructures* (Cambridge University Press, Cambridge, 2001).
[44] P. Palinginis and H. Wang, Appl. Phys. Lett. **78**, 1541 (2001).
[45] U. Woggon, *Optical Properties of Semiconductor Quantum Dots*, Vol. 136 of *Tracts in Modern Physics* (Springer, Berlin, 1996).
[46] T. Kuhn, in *Theory of Transport Properties of Semiconductor Nanostructures*, edited by E. Schöll, Vol. 4 of *Electronic Materials* (Chapman & Hall, London, 1998), Chap. 6, pp. 173–214.
[47] J. Fricke, V. Meden, C. Köhler, and K. Schönhammer, Ann. Phys. (N.Y.) **235**, 177 (1997).
[48] L. Mandel and E. Wolf, *Optical Coherence and Quantum Optics* (Cambridge University Press, Cambridge, 1995).
[49] V. M. Axt, M. Herbst, and T. Kuhn, Superlattices Microstruct. **26**, 117 (1999).
[50] J. J. Baumberg, D. A. Williams, and K. Köhler, Phys. Rev. Lett. **78**, 3358 (1997).
[51] P. Hawker, A. J. Kent, and M. Henini, Appl. Phys. Lett. **75**, 3832 (1999).
[52] R. Bellingham, A. J. Kent, A. V. Akimov, and M. Henini, Phys. Status Solidi B **224**, 659 (2001).
[53] L. Jacak, P. Machnikowski, J. Krasnyj, and P. Zoller, Eur. Phys. J. D **22**, 319 (2003).